



Automated Detection of Cardio Vascular Disease using Enhanced KNN classifier based on Sand Piper Optimization Algorithm

K. Kalamani^{1*}, D. Brindha²

¹*Professor, Department of Electronics and Communication Engineering, Coimbatore Institute of Engineering and Technology, Coimbatore: 641109, Tamil Nadu, India*

²*Associate Professor, Department of Electronics and Communication Engineering, Coimbatore Institute of Engineering and Technology, Coimbatore: 641109, Tamil Nadu, India*

*Corresponding author email: kalaimaniswetha@gmail.com

Abstract: In this manuscript recognition cardio vascular disease (CVD) is detected based on sand piper optimized with Enhanced KNN classifier is proposed. In this method the images are taken from the various data sets of the cardiac images are taken to excerpt the features of the images calculated using left ventricle (LV), end – diastolic volume (LVEDV), and end–systolic volume (LVSEV). In this proposed algorithm shows the optimal accuracy and computational performance for myocardial mass, wall thickness, left ventricle (LV) and right ventricle (RV) volume and ejection fraction (EF). The accuracy of the proposed Enhanced KNN classifier and Sand Piper Optimization (SPO) algorithm method shows the accuracy 6.45%, sensitivity shows 7.65%, Specificity shows 3.67%. F-measure shows the 12.56%, Recall shows the 7.89%, shows higher outputs when comparing with existing methods like Random Forest Classifier (RFC) and principle component analysis (PCA) respectively.

Keywords: Cardiovascular diseases (CVD), Magnetic resonance image (MRI), Sandpiper optimization algorithm, Enhanced KNN classifier.

1. INTRODUCTION

Currently heart disease is the main problem and it will cause death rate also high [1]. Coronary artery disease (CAD) [2], like angina and dead myocardial tissue [3,4], cause heart attack, stroke, heart disappointment, cardiac arrhythmia, hypertensive coronary disease, cardiomyopathy, coronary artery disease rheumatic disease, congenital coronary artery disease, aortic aneurysms, coronary valvular disease,

carditis, venous thrombosis, thromboembolic disease and peripheral disease provide path disease to integrate into CVD [5]. In Cardiovascular disease (CVD) [6] two groups of disease are analyzed using modals in coronary artery disease, they are invasive and non–invasive methods [7,8]. The images in catheter- based fit to invasive techniques [9, 10] and the images in the non-catheter- based belongs to the non- invasive image model [11,12]. In certain clinical cases, multiple images are obtained in dissimilar points in time or from different points of view [13, 14].



The ML and AI methods are conceivable to sustainance doctors to analyze and to compute accurate value of the patient in time [15,16]. These approaches can recover the ability of doctors and researchers to recognize and then examine the basic difference that cause disease. These procedures collected from conventional algorithms like Support Vector Machine (SVM), Neural Network (NN), and deep learning algorithms as Convolution Neural Network (CNN). These algorithms prime to numerous levels of concept, image and data routinely from huge set of images that demonstrate the preferred performance of figures [17].

The main objective of this manuscript sand piper algorithm is proposed to optimize Cardio vascular disease. In this segmenting process the heart image is taken from cardio vascular magnetic resonance imaging (MRI) and approximations from the specific dataset is intended using left ventricle (LV), end – diastolic volume (LVEDV), and end- systolic volume (RVESV) [18].

The major contributions of this manuscript are summarized below:

- Here, an automatic CMR image examination, utilise an Enhanced KNN based Sand Piper Optimized [19] Algorithm is proposed.
- The efficiency of the system has been appraised with a number of mechanical metrics, involving Dice metric, mean contour and Hausdorff distance, and clinically relevant measures with LV, RVEDV and RVESV [20].

Remaining manuscript is mentioned as below. The Literature survey is described in section 2. Section 3 A proposed Segmentation methods based on sand piper optimized Enhanced KNN classifier for cardiovascular disease (CVD). Result and discussion are suggested on section 4 and at last, Section 5 concludes the manuscript.

2. LITERATURE SURVEY

In 2017, *Mai et.al* [21] introduced improved wearable and mobile technology interventions for diminishing sedentary behavior and heart problems. It was used to estimate the efficiency of enhanced experience interferences aimed at eliminating sedentary behavior (SB) on healthy adults and to observe the behavior change techniques (BCT) utilized. The experimental results show that the gears of mobile and wearable technology caused an average reduction of -41.28 min per day (min / day).

In 2019, *Srivastava et.al* [22] presented effective prediction of heart disease with hybrid machine learning techniques. This method was used to predict the important structures by using machine learning systems that allow the precision on calculation of cardiovascular diseases to be tamed. The experimental results show that accuracy level of 88.7% performed by prediction model of heart disease through the hybrid random forest with linear model (HRFLM).

In 2020, *Acharya et.al* [23] have presented a deep

genetic set of classifiers for the detection of arrhythmias with ECG signals. This method was used to implement a three-layer (48 + 4 + 1) deep genetic ensemble of classifiers (DGEC). The advanced technique was a hybrid associating (1) joint learning, (2) deep learning, and (3) evolutionary computing. The developed DGEC system achieved a recognition of accuracy = 99.37%, specificity = 99.66% with single sample classification time = 0.8736 (s) in the detection of 17 ECG classes of arrhythmia.

In 2017, *Mahdi, et.al* [24] has presented a feature-based classifier and convolutional neural networks for detecting arrhythmias of short ECG segments. This method was used to implement the cardiovascular diseases using atrial fibrillation (AF) was extensive and exclusive. Then the experimental results show that convolutional neural network scored 72.1% in improved database and 83% in the test set.

In 2017, *Asl et al* [25] have presented an automated diagnosis of patients with coronary artery disease (CAD) with optimized SVM. This technique was used to implement the method for automatic examination of ordinary and coronary artery disease conditions by heart rate variability (HRV) signal removed as electrocardiogram (ECG). The principal component analysis (PCA) was applied for decreasing the number of features. The Support Vector Machine (SVM) classifier has been used for classifying two classes of data with extracted distinctive features.

In 2017, *Wang et al* [26] have presented a Detection of cardiovascular diseases from mammograms with deep learning. Coronary artery disease mainly affect the women to diagnose this disease Breast arterial calcifications (BACs), method was used. The result of this method shows linear regression with a coefficient of determination of 96.24%.

3. PROPOSED DETECTION METHOD BASED ON SAND PIPER OPTIMIZED ENHANCED KNN CLASSIFIER FOR CARDIOVASCULAR DISEASE (CVD)

In this section Detection method based on sand piper optimized Enhanced KNN classifier is explicated for the detection of CVD using MRI image. From figure 1 shows the block diagram for detecting the cardiovascular disease, the Left ventricle and right ventricle cardiac image is taken as the input and the image is taken by the process of magnetic resonance image (MRI) method. In this the input image is used to detect the cardio vascular disease (CVD) in the heart and to analyzes in the feature extraction. Then feature extraction process is takes place by using the sand piper optimized fully deep convolutional neural network. This process is used to detect the diseases in the heart. In this, a cavity is detected in the input image and then the image is partitioned into a series of semantically or automatically significant regions, interms of quantitative measures that may be removed like myocardial mass, wall



thickness, LV volume, RV volume, and ejection fraction (EF), so on. To detect CVD in heart the existing method shows less accuracy, to get more accuracy Enhance KNN classifier is used. Then to get more optimal solution the optimization problem sandpiper optimization algorithm (SPO) is proposed.

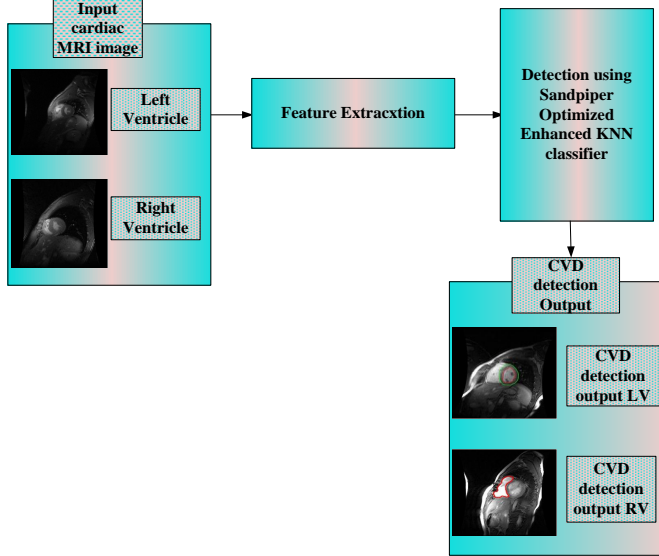


Figure 1: Block diagram for the detection of cardiovascular disease (CVD)

Enhanced KNN classifier model has two methods namely training and testing stages to test the cardiac image data. To test the image, cardiac images are taken to detect the Cardiovascular disease (CVD) and the images are cropped center by utilizing 256×256 pixel dimensions. The cardiac magnetic resonance image introduces a dataset with heart and the circulatory tissues of the human body. To decrease the computational difficulty in time and to recover the accuracy. In this find the location of LV and RV. Here to decrease the computational difficulty in the input image size that is 256×256 after reducing the image size then consider 64×64 it is the input.

Then observe the pixel coordinates of the top left and the bottom right of the images is $[1,1]$ and $[64,64]$. Then the convolved MRI image character computes the value is denoted in equation 1

$$L_o[a,b] = h(w_o[a,b]) \quad (1)$$

Where

$$w_o[a,b] = \sum_{C_p=1}^{11} \sum_{C_p=2}^{11} H_o[D_1 D_2] A[a + D_1 - 1, b + D_2 - 1] + x_0[o] \quad (2)$$

In this $i[a]$ represents the a -th component of vector I and $w_o[a,b]$ signifies the component a -th row and b -th column of matrix I .

Then the convolved characteristics of the image does not crash with neighbors through size 6×6 is calculated as

$$P_o[a_1, b_1] = \frac{1}{6} \sum_{x=(6x_1-5)}^{6x_1} \sum_{v=(6x_1-5)}^{6j_1} L_o[a, b] \quad (3)$$

Then the output can be calculated as the original cardio multi resonance image 256×256 is up sampled to 32×32 .

3.1 Enhanced K-Nearest Neighbor classifier (EKNN)

In this Enhanced KNN classifiers are used to determine the training set of cardiac images. In this process the trained images are calculated by using the n and m image features. Then the image features are calculated as

$$D = \left\{ \begin{array}{c} \sum_{w=1}^r N_w^1, \sum_{w=1}^r N_w^2, \dots, \sum_{w=1}^r N_w^v \\ r, r, \dots, r \end{array} \right\} \quad (4)$$

Where D represents the class center in the measured V diministic features space, r is the number of examples in the class, N_w^j is the data of j -th dimension of the w -th example. Then the strength of the item L_i is formulated as

$$JH(L_i) = \frac{[\chi * JH_A(L_i) + \delta * JH_B(L_i)]}{2} \quad (5)$$

Where $JH(L_i)$ represents the strength of the item L_i , and it is the weight average of two values. And it is the strength of the image in the class and it is denoted as $JH_A(L_i)$. Then the image is close to each other and it is denoted as $JH_B(L_i)$. χ and δ are the weighting factors to calculate the computational complexity respectively. Then the $JH_A(L_i)$ and $JH_B(L_i)$ is calculated as

$$JH_A(L_i) = \sum_{i \neq M} \frac{1}{EDIST(L_i, L_m)} \quad (6)$$

$$JH_B(L_i) = \sum_{i \neq M} \frac{1}{EDIST(L_i, D)} \quad (7)$$

Where $JH_A(L_i) = \sum_{i \neq M} \frac{1}{EDIST(L_i, L_m)}$ is the computational

complexity and $JH_B(L_i) = \sum_{i \neq M} \frac{1}{EDIST(L_i, D)}$ is the cost time of image complexity. Then the Euclidian distance with in the image L_i and L_M are represented by the below equations such as

$$EDIST(O_a, O_b) = \sqrt{\sum_{j=1}^v (O_a^j - O_b^j)^2} \quad (8)$$

Where O_a^j and O_b^j is the value of the j^{th} dimension of the points O_a and O_b in the v dimensional feature space. Then the computation complexity and time are calculated as by substituting equation 5 in 8 and it is given as

$$JH(L_i) = \frac{\left[\chi \sum_{i \neq M} \frac{1}{EDIST(L_i, L_m)} + \frac{\delta}{EDIST(L_i, D)} \right]}{2} \quad (9)$$

Equation 9 is known as the computational complexity and time cost. The faults in the Enhanced KNN classifier are, it requires more recall expenditures when large amount of data is to be in progress. The myocardial infraction for Enhanced KNN classifier shows the accuracy 0.67%. To get more accuracy and optimization technique is proposed in sandpiper optimization algorithm technique.

In this Sandpiper optimization (SPO) algorithm is proposed to decrease the cardiovascular disease (CVD) and to reduce the death of the human being. CVD is most dangerous disease and can stop the human life. Coronary artery diseases (CAD) like angina and dead myocardial tissue cause heart attack, stroke, heart disappointment, cardiac arrhythmia, hypertensive coronary disease, cardiomyopathy, rheumatic coronary disease, congenital coronary disease, aortic aneurysms, Coronary valvular disease, carditis, venous thrombosis, thromboembolic disease and peripheral disease provide a route of integration in CVD. While detecting Cardiovascular disease (CVD) using MRI image segmentation causes dangerous or serious process in real life heart cardiovascular performance metrices. To overcome the cardiovascular problem in human heart here proposed a novel algorithm called sand piper optimization algorithm. This algorithm is used to solve the above problem and give challenge to the real-life problems. Using sandpiper algorithm can find the causes of attacking behavior of the human body. This algorithm is used to execute by using two processes such as highlight intensification and diversification of the searching area. In this algorithm the experimental result shows the computational difficulty and convergence performance is calculated. Then sand piper algorithm use machine – learning algorithm to enhance the real-life results. It will

reduce the costs, danger, and increase the reliabilities.

1 Step by Step procedure

In this section have to discuss the segmentation process in medical images using Sandpiper algorithm reduce the cardiovascular diseases during the segmentation process. The step-by-step procedure shows the inspiration and computational representation of the proposed algorithm. This method is used to enhance the diagnosis and treatment of cardiac diseases and to reduce the death rate of CVD. This algorithm is calculated by using the distinct positions. Sandpipers may attack the particular position of the image and given to real life. This algorithm estimates the movement of the image from one position to another, during this process sand piper algorithm is used to clarify the distance. The proposed sandpiper optimization algorithm shows step by step procedure to solve the CVD is as follows:

Step 1: Initialization

Initialize the initial position of sandpipers to detect the MRI image and to find the cardiovascular disease from the heart, and detect the faults of this disease. Sand piper optimization algorithm is proposed to get optimized values with greater accuracy. During this movement's error may occur to minimize that errors and piper optimization is proposed from the following equations:

Here initialize the population \vec{L}_{bp} as the best searching term to detect cardiac disease and the below equation becomes

$$\vec{L}_{bp} = L_Y \times \vec{K}_{bs}(w) \quad (7)$$

Where L_Y is the collision avoidance, \vec{L}_{bp} is the positions of the searching term that will not collides between additional the searching criteria, $\vec{K}_{bs}(w)$ denotes the present position of searching criteria, q denotes the present iterations in searching area.

$$L_Y = L_h - (w \times L_h / iter_{Max}) \quad (8)$$

$$\text{Where, } w = 0, 1, 2, \dots, iter_{Max} \quad (9)$$

Where L_h denotes the controlling frequencies to change the variable L_Y is linear lower from L_h to 0, and if limitation $L_Y = 2$ i.e. assuming, the variables will lesser from 2 to 0 and then the value is 2 then the step is going on up to assuming the values.

Step 2: Random generation

After the collision avoidance process then to converge the



probing measures near the way of best neighbors. \overrightarrow{K}_{xBy} are the best probing measures and the equation is given below.

$$\overrightarrow{M}_{by} = L_X \times (\overrightarrow{K}_{xvr}(w) - \overrightarrow{K}_{bt}(w)) \quad (10)$$

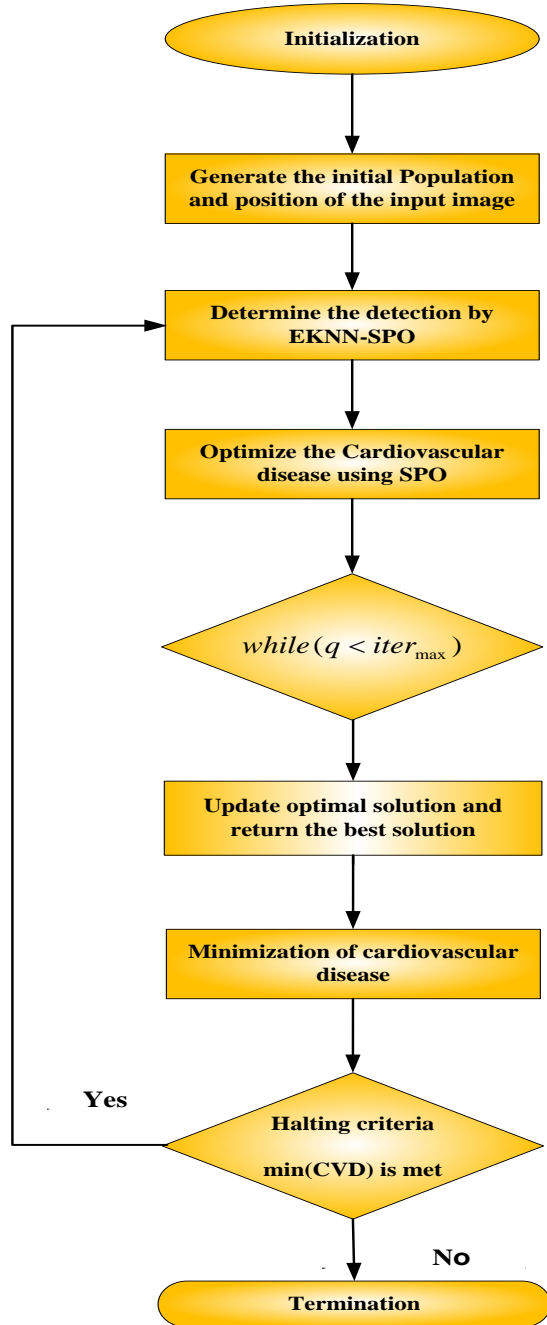


Figure 2: Flow chart for CVD

L_{Acc} is the random variable and it is responsible for better accuracy L_{Acc} Is derived as:

$$L_{Acc} = 0.5 \times Q_{rand} \quad (11)$$

Where W_{rand} a random number is lies on range of [0, 1].

Step 3: Fitness Function

From the initialized values, the random number of solutions is created. The fitness function of solution is evaluated and the objective function is represented in an optimization of function β in equation (6).

Step 4: Update the position using sand piper optimization (SPO) algorithm

In this step , SPO assigns the current best solution for the cardio vascular disease (CVD). Sandpiper is used to optimize the CVD and gives the best probing measures for the optimization.

Then update the position by sand piper’s optimization behavior using the following equation (13) probing measures are derived as:

$$\overrightarrow{N}_{bp} = \overrightarrow{L}_{bk} + \overrightarrow{V}_{bl} \quad (12)$$

Substitute equation 7 and 10 in equation 12 to update the space and to measure the CVD.

$$\overrightarrow{N}_{yl} = \overrightarrow{L}_{bk} + \overrightarrow{V}_{bl} + L_A \times L_X \times (\overrightarrow{K}_{xvr}(w) - \overrightarrow{K}_{bt}(w)) \quad (13)$$

Where \overrightarrow{N}_{yl} denotes the space in the CVD measures and the excellent right probing measures.

At the position of the detection the sandpiper may change its position and angle and to analyze the correct position to examine the images at entire points over the cardiac cycle. Then Sand pipers can generates the spiral behaviour to analyze the image. Then the 3-dimensional view of the cardiac cycle is given below:

$$J' = Q_{radius} \times \text{sinc}(a) \quad (14)$$

$$F' = Q_{radius} \times \cos c(a) \quad (15)$$

$$W' = Q_{radius} \times a \quad (16)$$

$$q = r \times \beta^{cj} \quad (17)$$

Where, Q_{radius} denotes the radius of every spin, a is the variable lie in the range of $[0 \leq C \leq 2\pi]$ t and a denote the spiral shape constant and β denotes the base of the natural algorithm. Then consider the values j and r is 1 and it behave as constant then the updated equation is (19)



Step 5: Minimization of cardiovascular disease

Let us consider the constant values $u.j. = 1$ then the shape of the image become complex. So, the position is updated as

$$\vec{N}_{yl}(w) = (\vec{F}_{yl} \times (j' + f' + w')) \times \vec{N}_{ayl}(q) \quad (18)$$

Where $\vec{N}_{yl}(w)$ minimize the cardiovascular disease using magnetic resonance heart image and gives the best solution for the sandpiper optimization algorithm.

Step 6: Termination

The sandpiper optimization algorithm optimizes the disorders in the cardiovascular diseases in heart using equation 18; here both the objective functions and constraint functions are taken from magnetic resonance image and used to find the disorders in the heart. Finally, the outputs of sandpiper optimization (SPO) algorithm are achieved by minimizing the cardiovascular diseases in heart based on Enhanced KNN Classifier, and the performance metrics are shown in table 1.

4. RESULT AND DISCUSSION

In this section, the simulation performance of proposed to Enhance KNN classifier interms of Sandpiper optimization algorithm is used to optimize the CVD. Here the presentation metrics has been estimated using the technical metrics, such as Dice metric, mean contour and Hausdorff distance, for the clinically refer to LV, LVEDV, RVEDV and RVESV. The MATLAB simulations are performed on PC with the Intel Core i5, 2.50 GHz CPU, 8GB RAM and Windows 8. All simulation programs are implemented. Here proposed the accuracy, specificity, sensitivity, F-measure, Recall are performed in the cardiac disorders. Then the performance of the proposed method Sandpiper optimization algorithm (SPO) gives better result when compared with existing method such as Random Forest Classifier (RFC) and principal component analysis (PCA).

5.1 Evaluation Metrics

In this paper, different performance measures are used to calculate the results. The accuracy, are evaluated in allocation task for the proposed CBIR framework. The above-mentioned terms are calculated as,

$$\text{Accuracy } K_A = 0.5 \times W_{rand} \quad (19)$$

Where W_{rand} a random number is lies on range of [0, 1].

5.1.1. Dice metrics

The dice metric can be calculated in the automated

segmentation B and manual segmentation A and the equation can be derived as follows:

$$D.M = \frac{2|X \cap Y|}{|X| + |Y|} \quad (20)$$

The above equation 7 denotes the values between the 0 and 1. Then 0 denote no collision and 1 denotes perfect agreement.

5.5.2. Mean contour distance

Consider, y_b and y_a are the dice surfaces equivalent to two binary segmentation masks b and a. The mean counter distance (MD) is defined as:

$$M.D = \frac{1}{2} \left(\frac{1}{N_y} \sum_{l \in y_b} e(P, B_a) + \frac{1}{N_b} \sum_{z \in y_a} e(P, B_y) \right) \quad (21)$$

5.1.3. Hausdorff distance (HD)

Then the Hausdorff distance (HD) is defined as:

$$H.D = \text{Maxi}(\text{Maxi}_{l \in y_b} e(P, B_x), \text{Maxi}_{z \in y_a} e(x, B_y)) \quad (22)$$

Where, $e(P, B_x) = \min_{z \in y} i e(P, x)$ denotes the minimum

distance of point l from the points. Then the mean distance and the Hausdorff distance calculate the largest distance among two surfaces and it is very sensitivity. From equation 7 and 8 the mean counter and Hausdorff distance is calculated and the maximal distance at point Y and the segmentation counter Y_b and Y_a .

5.1.4. Ejection Fraction

Ejection Fraction (EF) is a vital cardiac parameter to identify the cardiac output. And it is defined as

$$EF = \frac{EDV - ESV}{EDV} \times 100\% \quad (23)$$

Where EDV implies end – diastolic volume and ESV implies end systolic volume.

5.1.5. myocardial Mass

The myocardial mass (M. mass) and myocardial volume (M. volume) is defined as

$$M.\text{mass} = M - \text{volume}(\text{cm}^3) \times 1.06(\text{gram}/\text{cm}^3) \quad (25)$$

Then the performance metrics shows the LV, LVEDV, and



LVESV, LVM; RV, RVEDV and RVESV.

5.2. Simulation Phase 1: MRI Medical Image for Cardiovascular disease (CVD)

The below figure 3 shows the segmented image for the cardio vascular disease using magnetic resonance image (MRI) [29, 30]. The segmentation process is done by using the proposed algorithm namely sandpiper optimization algorithm. The below figure shows that automated segmented MRI image.

The segmented images are calculated by using the Dice metric, mean contour and Hausdorff distance for Left ventricle. In this the Left ventricle end diastolic volume, left

ventricle End systolic volume are diagnosed using MRI image technique by using sand piper optimization (SPO) algorithm. The input image shows the Left ventricle MRI image shows the abnormalities in the left ventricle wall position then the image is diagnosed during the End diastolic volume, then also a cavity is found in the wall of the heart and then diagnosed the wall after segmentation process. After analyzing the End Systolic wall thickness of the heart, the cavity is found that is recognized and diagnosed using the sand piper optimization algorithm. Then the image variations are calculated by using fully deep convolution Network, Deep convolution filters, Dice metric, mean contour and Hausdorff distance.

| Input image | Left Ventricle | LVEDV | LVSEV | Output image |
|---|---|---|--|---|
|  |  |  |  |  |
|  |  |  |  |  |
|  |  |  |  |  |
|  |  |  |  |  |
|  |  |  |  |  |
|  |  |  |  |  |
|  |  |  |  |  |

Figure 3: Shows the segmentation figure for Left ventricle





Figure 4: shows the segmentation figure for Right ventricle

The figure 4 shows the segmented image for the cardio vascular disease using magnetic resonance image (MRI).

The segmentation process is done by using the proposed algorithm namely sandpiper optimization algorithm. The below figure shows the automated segmented MRI image. The segmented images are calculated by using the Dice metric, mean contour and Hausdorff distance for Left ventricle. In this the Left ventricle end diastolic volume [31], Left ventricle End systolic volume are diagnosed using MRI image technique by using sand piper optimization (SPO) algorithm. The input image shows the Left ventricle MRI image shows the abnormalities in the left ventricle wall position then the image is diagnosed during the End diastolic volume, then also a cavity is found in the wall of the heart and then diagnosed the wall after segmentation process. After analyzing the End Systolic wall thickness of the heart, the cavity is found that is recognized and diagnosed using the sand piper optimization algorithm. Then the image variations are calculated by using fully deep convolution Network, Deep convolution filters, Dice metric, mean contour distance and Harsdorff distance.

5.3. Simulation Phase 1: Performance Comparison of various methods

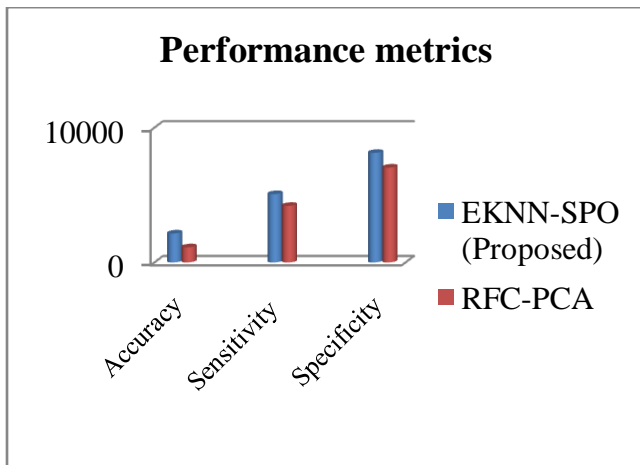


Figure 5: Performance Metrics

Figure 5 shows the existing method such as RFC and PCA, set the proposed sandpiper optimization (SPO) Shows the better performance metrics in Accuracy, Sensitivity, Specificity. At the node Accuracy, the proposed sandpiper optimization (SPO) algorithm shows the Accuracy, 3.1%, 6.45%, 6.0%, 4.21% higher than the Existing RFC and PCA set the proposed sandpiper optimization (SPO). At the node sensitivity the proposed sandpiper optimization (SPO) algorithm shows the Sensitivity, 5.55%, 4.39%, 2.15%, 5.55% higher than the RFC and PCA, set the proposed sandpiper optimization (SPO). At the node Specificity, the proposed sandpiper optimization (SPO) algorithm shows the Specificity, 6.59%, 8.98%, 5.43%, 2.10% higher than the Existing RFC and PCA, set the proposed sandpiper optimization (SPO)respectively.

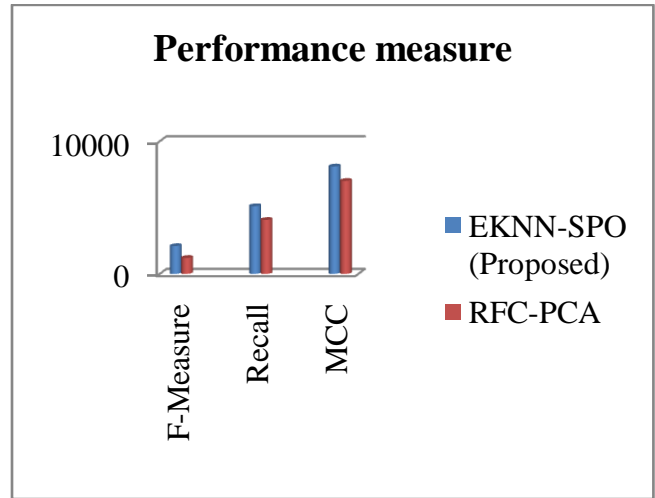


Figure 6: Performance Metrics

Figure 6 shows the existing method such as RFC and PCA, set proposed sandpiper optimization (SPO) Shows the better performance metrics in F-measure, Recall, Matthews correlation coefficient (MCC). At the node F-measure, the proposed sandpiper optimization (SPO) algorithm shows the F-measure, 8.79%, 12.5%,10%,16.47% higher than the Existing RFC and PCA, set the proposed sandpiper optimization (SPO). At the node Recall the proposed sandpiper optimization (SPO) algorithm shows the Recall, 8.13%, 12.04%, 14.81%, 3.33% higher than the RFC and PCA set the proposed sandpiper optimization (SPO). At the node Matthews correlation coefficient (MCC), the proposed sandpiper optimization (SPO) algorithm shows the Matthews correlation coefficient (MCC), 15.18%, 12.34%, 13.75%,21.33% higher than the Existing RFC and PCA, set the proposed sandpiper optimization (SPO)respectively.

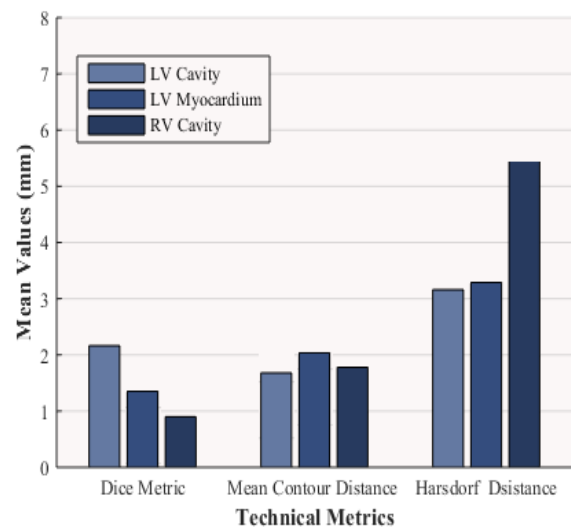


Figure 7: Technical Metrics and mean values



Figure 7 shows the proposed sandpiper optimization (SPO) for Technical metrics in Dice metric, Mean Contour and Hausdorff Distance. From this graph the various technical measures of Dice metric of LV cavity is higher than LV myocardium mass and RV. Then the Mean contour distance shows the Left ventricle myocardium mass is higher than the Left ventricle cavity and Right ventricle cavity. Then the Harsdorf Distance shows the Right ventricle cavity is higher than the Left ventricle cavity and myocardium mass and comparing with existing methods such as RFC and PCA, set the proposed sandpiper optimization (SPO) respectively.

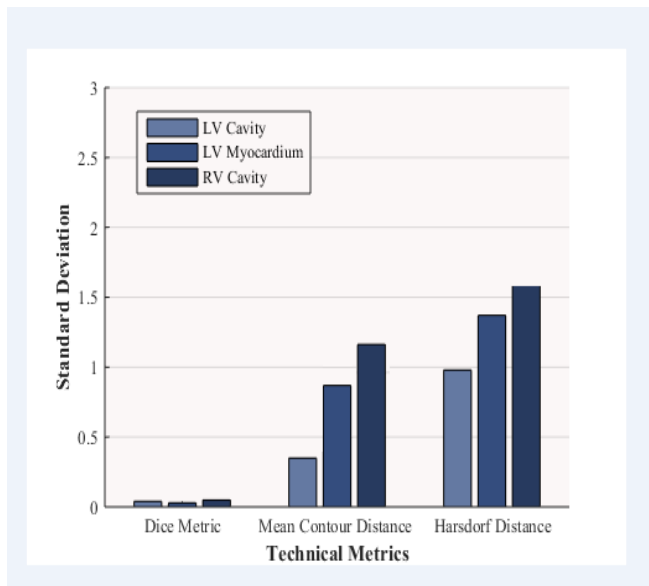


Figure 8: Technical Metrics and standard Deviation

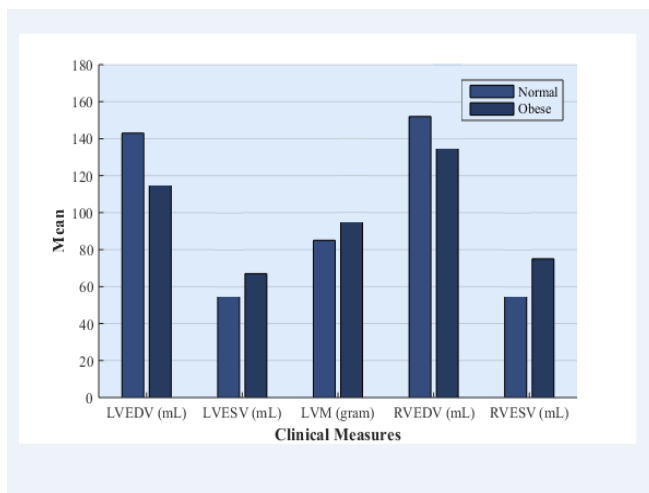


Figure 9: Clinical Measures and mean

Figure 8 shows the proposed sandpiper optimization (SPO) for Technical metrics in Dice metric, Mean Contour and Hausdorff Distance. From this graph the various technical measures of Dice metric of LV cavity is higher

than LV myocardium mass and RV. Then the Mean contour distance shows the Right ventricle cavity is higher than the Left ventricle cavity and myocardium mass. Then the Harsdorf Distance shows the Right ventricle cavity is higher than the Left ventricle cavity and myocardium mass and comparing with existing methods such as RFC and PCA, set the proposed sandpiper optimization (SPO) respectively.

Figure 9 shows the existing method such as RFC and PCA set the proposed sandpiper optimization (SPO) shows the improved Technical metrics and mean. At node the Left Ventricle End systolic volumes lower than the obese person. The LV Mass is lower than the obese person. The RVEDV is higher than the obese person. The LVESV is lower than the obese person, comparing with existing methods such as RFC and PCA, set the proposed sandpiper optimization (SPO) respectively.

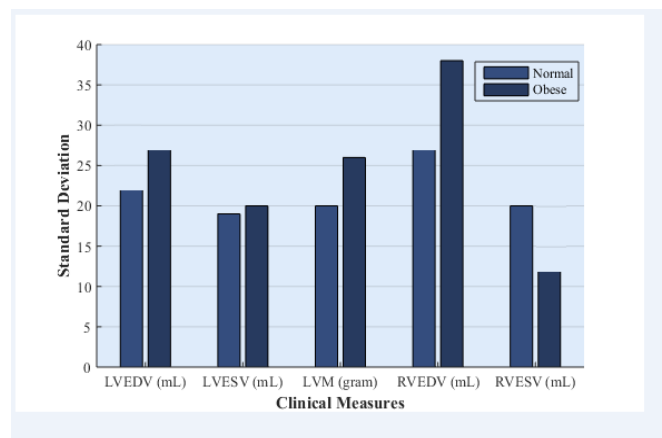


Figure 10: Clinical Measures and Standard deviation

From figure 10 shows the existing method such as RFC and PCA set the proposed sandpiper optimization (SPO) shows the improved Technical metrics and standard deviation on LVEDV, LVESV, LVM, RVEDV, and RVESV. From the graph, for the normal person at node The LVEDV is lower than the obese person. At node the LVESV is lower than the obese person. The LV Mass is lower than the obese person. The RVEDV is lower than the obese person. The LVESV is higher than the obese person, comparing with existing methods such as RFC and PCA set the proposed sandpiper optimization (SPO) respectively.

Figure 11 shows the manual mode of proposed sandpiper optimization (SPO), shows the better clinical measures and mean in Left ventricle stroke volume, left ventricular ejection fraction, left ventricular cardiac output, Right ventricular stroke volume, Right ventricular Ejection fraction, Right ventricle cardiac output. At node Left ventricle stroke volume, the manual observation is higher than the observation 1, 2, 3. At the node Left ventricle ejection fraction the manual observation is higher than the observation 1, 2, 3. At the node Left ventricle cardiac output the manual and observation value is equal when compare



with observation 1, 2. At the node Right ventricle stroke volume the observation 1 is higher than the manual output and observation 2, 3. At the node Right ventricle ejection fraction observation 3 is higher than the manual output and observation 1, 2. At the node Left ventricle cardiac output the manual output is higher than the observation 1,2,3 and comparing with existing methods such as RFC and PCA, set the proposed sandpiper optimization (SPO) respectively.

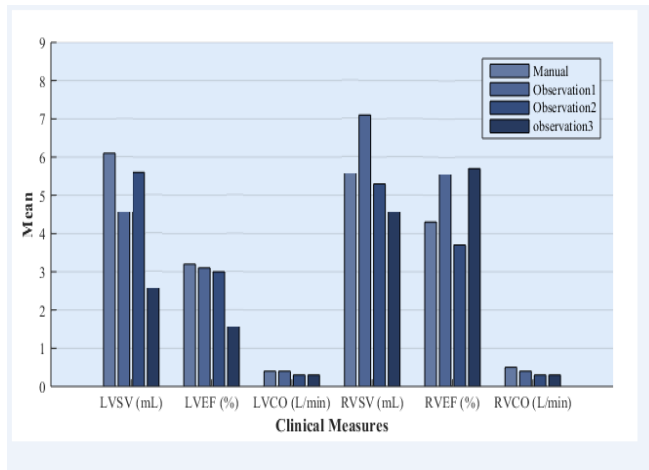


Figure 11: Clinical Measures and mean

5. CONCLUSION

In this paper, to detect the Cardio vascular Diseases (CVD) in Heart is identified by the method Enhanced KNN Classifier using the proposed algorithm known as Sandpiper optimization algorithm (SPO) in clinical basis. In this, the use of CVD- MRI image is taken as the input image then the disease is optimized using Sand piper optimization algorithm. The complications in LVEDV, LVESV, LVM, RVEDV, RVESV are optimizes using the proposed method sandpiper algorithm (SPO). In this a cavity is noticed and that cavity is diagnosed using this method and then the image is analyzed using Dice metric, mean contour, and Hausdorff distance Method. The experimental outcomes demonstrate that proposed system sandpiper shows the better performance such as accuracy of proposed system shows the 3.56%, sensitivity shows 6.45%, Specificity shows 8.554%. F-measure shows the 4.556%, Recall shows the 9.57%, for compared with different nodes when compared with the existing method RFC and PCA set the proposed sandpiper optimization (SPO) respectively.

REFERENCES

1. F. Yu, N. Selva Kumar, D. Choudhury, L. Foo and S. Ng, **Microfluidic platforms for modeling biological barriers in the circulatory system**, *Drug Discovery Today*, vol. 23, no. 4, pp. 815-829, 2018. Available: 10.1016/j.drudis.2018.01.036.
2. S. Hamada, D. Kashiwazaki, S. Yamamoto, N. Akioka, N. Kuwayama and S. Kuroda, **Impact of Plaque Composition on Risk of Coronary Artery Diseases in Patients with Carotid Artery Stenosis**, *Journal of Stroke and Cerebrovascular Diseases*, vol. 27, no. 12, pp. 3599-3604, 2018. Available: 10.1016/j.jstrokecerebrovasdis.2018.08.031.
3. L. Bavia, K. Lidani, F. Andrade, M. Sobrinho, R. Nisihara and I. de Messias-Reason, **Complement activation in acute myocardial infarction: An early marker of inflammation and tissue injury?**, *Immunology Letters*, vol. 200, pp. 18-25, 2018.
4. M. Slavich, G. Pizzetti, A.M. Vella, C. Carlucci, D. Margonato, R. Spoladore, G. Fragasso, and A. Margonato, **Extracorporeal myocardial shockwave therapy; a precious blast for refractory angina patients**, *Cardiovascular Revascularization Medicine*, vol. 19, no. 3, pp. 263-267, 2018. Available: 10.1016/j.carrev.2017.09.018.
5. H. Miptah, A. Ramli, M. Mohamad, H. Hashim and Z. Tharek, **Non-alcoholic fatty liver disease (NAFLD) and the cardiovascular disease (CVD) risk categories in primary care: is there an association?**, *BMC Family Practice*, vol. 21, no. 1, 2020. Available: 10.1186/s12875-020-01306-7
6. A. Gheorghe, U. Griffiths, A. Murphy, H. Legido-Quigley, P. Lamptey and P. Perel, **The economic burden of cardiovascular disease and hypertension in low- and middle-income countries: a systematic review**, *BMC Public Health*, vol. 18, no. 1, 2018. Available: 10.1186/s12889-018-5806-x
7. R. Alizadehsani, M.J. Hosseini, A. Khosravi, F. Khozimeh, M. Roshanzamir, N.Sarrafzadegan, and S. Nahavandi, **Non-invasive detection of coronary artery disease in high-risk patients based on the stenosis prediction of separate coronary arteries**, *Computer Methods and Programs in Biomedicine*, vol. 162, pp. 119-127, 2018. Available: 10.1016/j.cmpb.2018.05.009.
8. E. Makovac, J. Thayer and C. Ottaviani, **A meta-analysis of non-invasive brain stimulation and autonomic functioning: Implications for brain-heart pathways to cardiovascular disease**, *Neuroscience & Biobehavioral Reviews*, vol. 74, pp. 330-341, 2017. Available: 10.1016/j.neubiorev.2016.05.001.
9. P. Maury, P. Defaye, D. Klug, C. Alonso, F. Anselme, L. Fauchier, E. Gandjbakhch, D. Gras, J.S. Hermida, G.Laurent, and J. Mansourati, **Position paper concerning the competence, performance and environment required for the practice of ablation in children and in congenital heart disease**, *Archives of Cardiovascular Diseases*, vol. 113, no. 8-9, pp. 492-502, 2020. Available: 10.1016/j.acvd.2020.02.002 [
10. C. El-Hajj and P. Kyriacou, **A review of machine learning techniques in photoplethysmography for**



- the non-invasive cuff-less measurement of blood pressure, *Biomedical Signal Processing and Control*, vol. 58, p. 101870, 2020. Available: 10.1016/j.bspc.2020.101870
11. W. AlJaroudi and F. Hage, **Review of Cardiovascular Imaging in the Journal of Nuclear Cardiology in 2016. Part 1 of 2: Positron Emission Tomography, Computed Tomography and Magnetic Resonance**, *Journal of Nuclear Cardiology*, vol. 24, no. 2, pp. 649-656, 2017. Available: 10.1007/s12350-017-0820-4
 12. G. Verma, R. Kesharwani, P. Veeresh, H. Kaur, D. Sarmah, V. Kotian, L. Mounica, A. Borah, K. Kalia, and P. Bhattacharya, **Advances in Diagnostic Techniques for Therapeutic Intervention**, *Biomedical Engineering and its Applications in Healthcare*, pp. 105-121, 2019. Available: 10.1007/978-981-13-3705-5_5
 13. A. Lam, **Update on Adrenal Tumours in 2017 World Health Organization (WHO) of Endocrine Tumours**, *Endocrine Pathology*, vol. 28, no. 3, pp. 213-227, 2017. Available: 10.1007/s12022-017-9484-5.
 14. S. Kazemifar et al., **MRI-only brain radiotherapy: Assessing the dosimetric accuracy of synthetic CT images generated using a deep learning approach**, *Radiotherapy and Oncology*, vol. 136, pp. 56-63, 2019. Available: 10.1016/j.radonc.2019.03.026
 15. S. Fahle, C. Prinz and B. Kuhlenkötter, **Systematic review on machine learning (ML) methods for manufacturing processes – Identifying artificial intelligence (AI) methods for field application**, *Procedia CIRP*, vol. 93, pp. 413-418, 2020. Available: 10.1016/j.procir.2020.04.109
 16. F. García-Peñalvo and A. Mendes, **Exploring the computational thinking effects in pre-university education**, *Computers in Human Behavior*, vol. 80, pp. 407-411, 2018. Available: 10.1016/j.chb.2017.12.005
 17. M. Alkadri, M. Turrin and S. Sariyildiz, **A computational workflow to analyse material properties and solar radiation of existing contexts from attribute information of point cloud data**, *Building and Environment*, vol. 155, pp. 268-282, 2019. Available: 10.1016/j.buildenv.2019.03.057.
 18. M. Khened, V. Kollerathu and G. Krishnamurthi, **Fully convolutional multi-scale residual DenseNets for cardiac segmentation and automated cardiac diagnosis using ensemble of classifiers**, *Medical Image Analysis*, vol. 51, pp. 21-45, 2019. Available: 10.1016/j.media.2018.10.004.
 19. A. Kaur, S. Jain and S. Goel, **Sandpiper optimization algorithm: a novel approach for solving real-life engineering problems**, *Applied Intelligence*, vol. 50, no. 2, pp. 582-619, 2019. Available: 10.1007/s10489-019-01507-3.
 20. W. Shaban, A. Rabie, A. Saleh and M. Abo-Elsoud, **A new COVID-19 Patients Detection Strategy (CPDS) based on hybrid feature selection and enhanced KNN classifier**, *Knowledge-Based Systems*, vol. 205, p. 106270, 2020. Available: 10.1016/j.knosys.2020.106270.
 21. A. Stephenson, S. McDonough, M. Murphy, C. Nugent and J. Mair, **Using computer, mobile and wearable technology enhanced interventions to reduce sedentary behaviour: a systematic review and meta-analysis**, *International Journal of Behavioral Nutrition and Physical Activity*, vol. 14, no. 1, 2017. Available: 10.1186/s12966-017-0561-4.
 22. S. Mohan, C. Thirumalai and G. Srivastava, **Effective Heart Disease Prediction Using Hybrid Machine Learning Techniques**, *IEEE Access*, vol. 7, pp. 81542-81554, 2019. Available: 10.1109/access.2019.2923707.
 23. P. Pławiak and U. Acharya, **Novel deep genetic ensemble of classifiers for arrhythmia detection using ECG signals**, *Neural Computing and Applications*, vol. 32, no. 15, pp. 11137-11161, 2019. Available: 10.1007/s00521-018-03980-2.
 24. F. Andreotti, O. Carr, M. Pimentel, A. Mahdi and M. De Vos, **Comparing Feature Based Classifiers and Convolutional Neural Networks to Detect Arrhythmia from Short Segments of ECG**, *2017 Computing in Cardiology Conference (CinC)*, 2017. Available: 10.22489/cinc.2017.360-239.
 25. A. Davari Dolatabadi, S. Khadem and B. Asl, **Automated diagnosis of coronary artery disease (CAD) patients using optimized SVM**, *Computer Methods and Programs in Biomedicine*, vol. 138, pp. 117-126, 2017. Available: 10.1016/j.cmpb.2016.10.011.
 26. J. Wang et al., **Detecting Cardiovascular Disease from Mammograms With Deep Learning**, *IEEE Transactions on Medical Imaging*, vol. 36, no. 5, pp. 1172-1181, 2017. Available: 10.1109/tmi.2017.2655486.
 27. E. Cariou et al., **Diagnostic score for the detection of cardiac amyloidosis in patients with left ventricular hypertrophy and impact on prognosis**, *Amyloid*, vol. 24, no. 2, pp. 101-109, 2017. Available: 10.1080/13506129.2017.1333956
 28. D. Zentner et al., **A rapid scoring tool to assess mutation probability in patients with inherited cardiac disorders**, *European Journal of Medical Genetics*, vol. 61, no. 2, pp. 61-67, 2018. Available: 10.1016/j.ejmg.2017.10.020
 29. V.P. Kamphuis, J.J.M. Westenberg, R.L. van der Palen, N.A. Blom, A. de Roos, R. van der Geest, M.S. Elbaz, and A.A. Roest, **Unravelling cardiovascular disease using four dimensional flow cardiovascular magnetic resonance**, *The International Journal of Cardiovascular Imaging*, vol. 33, no. 7, pp. 1069-1081, 2016. Available: 10.1007/s10554-016-1031-9
 30. M. Modak, M. Frey, S. Yi, Y. Liu and E. Scott, **Employment of targeted nanoparticles for imaging**



- of cellular processes in cardiovascular disease, *Current Opinion in Biotechnology*, vol. 66, pp. 59-68, 2020. Available: 10.1016/j.copbio.2020.06.003
31. E. Chiodi, M. Nardoza, M.R. Gamberini, A. Pepe, M. Lombardi, G.Benea, and D. Mele, **Left ventricle remodeling in patients with β -thalassemia major. An emerging differential diagnosis with left ventricle noncompaction disease**, *Clinical Imaging*, vol. 45, pp. 58-64, 2017. Available: 10.1016/j.clinimag.2017.05.010.

